

Incommensurate structural phase transition in BaMnF₄: Light scattering from phasons

K. B. Lyons, R. N. Bhatt, T. J. Negran, and H. J. Guggenheim

Bell Laboratories, Murray Hill, New Jersey 07974

(Received 5 March 1981; revised manuscript received 22 July 1981)

We report an extensive series of optical investigations of BaMnF₄ near its incommensurate structural phase transition at $T_i \approx 254$ K. We observe an inelastic central peak in the range (247 ± 7) K. An anomaly occurs in the elastic scattered intensity at 241 K on heating, but the Raman peaks characteristic of the low-temperature phase persist up to 254 K. Measurements of the thermal diffusivity by a novel optical-electronic technique indicate that (1) the observed inelastic central peak is not due to entropy fluctuations, (2) the anomaly in the elastic central-peak intensity coincides with the peak in the pyroelectric coefficient, and (3) the value of pyroelectric coefficient changes sign within 1 K of T_i . The maximum in the inelastic central-peak intensity at 247 K may indicate another phase transition or may relate to the scattering mechanism. The anomaly in the elastic central peak is not a precise indicator of T_i , exhibits hysteresis, and may arise from static domain or defect scattering. The observed \bar{q} dependence of the inelastic central-peak width is consistent with an interpretation based on phason scattering and provides evidence for a strongly anisotropic, overdamped phason response in the incommensurate phase. Finally, we present evidence from detailed line-shape analysis that the observed intensity may actually be the result of coupling between the phason and the LA phonon.

I. INTRODUCTION

Structural phase transitions involving incommensurate distortions are currently of considerable interest. Although microscopic or phenomenological models exist for some of these systems,^{1,2} the incommensurate phase in BaMnF₄ remains incompletely understood. A detailed neutron scattering investigation provided the first evidence for an incommensurate phase in this material. Below the transition $T_i = 247$ K, the incommensurate distortion was observed to develop continuously at a wave vector $\bar{q}_0 = (0.392, 0.5, 0.5)$. However, despite careful investigation, the nature of the soft-mode eigenvector remained unknown. Even so, BaMnF₄ is especially interesting, since the high-temperature phase lacks inversion symmetry³ and exhibits pyroelectricity.⁴ This has important consequences for the use of light scattering to study the dynamics of the incommensurate phase. The reader may refer to the recent article by Scott⁵ for a detailed review of the other literature on BaMnF₄. In the present article we discuss mainly the light scattering studies performed near T_i by ourselves and other workers which bear on the issue of phason dynamics.

In Sec. II we review material particularly pertinent to light scattering. In Sec. III we describe the experimental apparatus and results for the various optical experiments performed. Further discussion and analysis of those results appear in Sec. IV.

II. BACKGROUND

To discuss the effects of inversion symmetry we must first note the peculiarities of the long-range order of an incommensurate structure.⁶ While the structure no longer exhibits true long-range periodicity, it may still do so to a good approximation when the incommensurate distortion is small. For example, a lattice with inversion symmetry in the parent phase will no longer have inversion symmetry about every lattice point in the distorted phase. However, in the infinite lattice one can always find a point with symmetry *arbitrarily close* to centrosymmetric. As Janner and Janssen⁶ have discussed at some length, the lattice still has inversion symmetry in that limiting sense in the incommensurate phase.

The incommensurate distortion also causes new "zone-center" vibrational modes to appear in the new quasiperiodic lattice. Although this is entirely analogous to the folding of zone-boundary modes into the zone center in the case of a commensurate cell-doubling phase transition, in the incommensurate case, modes of a new kind appear. Let us consider a single-plane wave (SPW) distortion of the type

$$\psi = \psi_0 e^{i\bar{k}_0 \cdot \bar{r}} e^{i\phi} . \quad (1)$$

For a commensurate cell-multiplying phase transition, \bar{k}_0 is commensurate with the parent lattice, and ϕ has a certain fixed equilibrium value. The fluctuations

$\delta\psi_0$ and $\delta\phi$ are thus *both* finite-energy excitations below T_i , even at $q=0$. Since, for the incommensurate case, in contrast, the equilibrium value of ϕ may vary arbitrarily, the fluctuations $\delta\phi$ have zero energy at $q=0$. The dispersion of this mode thus differs qualitatively from the related vibrations near commensurate phase transitions. This mode is called a phason, the direct spectral observation of which had, until very recently, eluded investigators. One of the fundamental questions about this new class of excitations is whether they are propagating or overdamped. Although an overdamped phason light scattering peak has been observed in BaMnF_4 ,⁷ an underdamped feature has been reported in neutron scattering observations at much higher \bar{q} in the case of biphenyl.⁸ We discuss the former case in detail in the present paper. It remains to be seen whether the overdamped character reported here for the $q \rightarrow 0$ phasons in BaMnF_4 is a general feature of incommensurate phases.

The low frequency anticipated for phasons makes light scattering a potentially attractive probe for their study, providing that they will indeed scatter light. Since the amplitude fluctuations $\delta\psi_0$ are strictly analogous to soft optic modes at commensurate phases transitions, they are always Raman active below T_i . If we now relate the atomic movements for the phason to those for a fluctuation $\delta\psi_0$, we can easily examine their light scattering activity. We write the set of atomic movements associated with a fluctuation $\delta\psi_0$ as

$$\delta u_\alpha^\psi(\bar{r}) \equiv \delta\psi_0 u(\alpha, \bar{r}) \quad (2)$$

for the unit cell at \bar{r} , where α enumerates the atoms within the unit cell. Since a change in ϕ corresponds to a displacement of the static distortion with respect to the lattice, we may write the atomic movements for $\delta\phi$ as

$$\delta u_\alpha^\phi(\bar{r}) \equiv \psi_0 \frac{\partial}{\partial x} u(\alpha, \bar{r}) \frac{\delta\phi}{k_0}, \quad (3)$$

where we have assumed $\bar{k}_0 \parallel \bar{x}$ in Eq. (1). From Eqs. (2) and (3), the effects of inversion symmetry are obvious. Analogous to the discussion above, if the parent phase is centrosymmetric, then we can choose an origin such that the quantities $u(\alpha, \bar{r})$ are even, under inversion, to an arbitrary precision. To the same precision, the quantities $\partial u(\alpha, \bar{r})/\partial x$ (then become odd under inversion. Since that mode (of odd parity) will *not* scatter light at $q=0$, the phasons represented by Eq. (3) may do so only if the *parent* phase lacks inversion symmetry. We note that phason scattering is always *Brillouin* allowed (i.e., $I \propto q^2$), but this effect may be small.

BaMnF_4 is an example of a noncentrosymmetric system which undergoes a transition to an incommensurate phase. Since, according to the discussion

above, its phasons should scatter light, it provides an ideal opportunity for direct observation of phasons.

Others have previously studied the light scattering spectrum of BaMnF_4 . After ultrasonic measurements⁹ first disclosed a phase transition at 247 K, Ryan and Scott¹⁰ and Popkov¹¹ demonstrated the presence of additional Raman lines in the low-temperature phase. Based on this evidence, they identified the transition as of zone-boundary type. In a Brillouin scattering investigation near the structural phase transition in BaMnF_4 , Bechtle and Scott^{12,13} demonstrated a strong dispersion near 1 GHz in a transverse acoustic velocity. About the same time, a comprehensive neutron scattering investigation¹⁴ demonstrated the incommensurate nature of the phase below T_i . Bechtle and Scott then suggested¹³ that the observed dispersion represented coupling between the transverse acoustic (TA) and phason modes near T_i . The anomaly in the elastic scattered intensity observed by Lockwood was found in a polarized $b(aa)c$ geometry. Bechtle, Scott, and Lockwood published these results jointly¹³ and applied the model describing the acoustic dispersion to the central-peak spectra. However, not only did the geometry of the two investigations differ fundamentally, but also the reported linewidths included no correction for the instrumental width.¹⁵ Since the latter represented at least 80% of the observed width, that interpretation¹³ of the central peak is questionable, and has been retracted in the more recent work¹⁵

Our initial experiments,¹⁶ demonstrated the existence of a polarized inelastic central-peak scattering near T_i . The peak exhibits a q -dependent width larger than predicted by the model of Bechtle *et al.* and exhibits a temperature dependence less singular than that reported by Lockwood¹³ for the elastic scattering.

After reevaluation of the data, Lockwood *et al.*¹⁵ concluded that the central-peak scattering they observed emanates from static centers ($\Gamma_{CP} \leq 0.3$ GHz). However, they also find intensity between the LA and mixed acoustic modes, and conclude that an additional imperfectly resolved phason peaks exists.¹⁵ In what follows, we shall present a rather different interpretation, supported by additional new experimental observations.

III. EXPERIMENT

The present work includes several different but related experiments. These include (by section number):

(III A) Spectral characterization of the central peak¹⁶ with simultaneous observation of the Brillouin and Raman scattering spectra in various geometries, mainly with $\bar{q} \parallel c$ and $\bar{q} \parallel a$. The intensities of the Raman peaks suggest a transition occurring at 254 K, 7°

above the temperature T_m at which the inelastic central-peak intensity is a maximum.

(III B) Thermal diffusivity measurements by a novel optical technique¹⁷ which show that entropy fluctuations do not cause the observed central-peak scattering. These measurements also provide evidence for a transition occurring at 254 K.

(III C) Further central-peak measurements, carried out for \vec{q} deviating from c in the ac plane by angles up to 26° , which demonstrate the presence of a strong anisotropy in the process responsible for the central-peak scattering.⁷ This anisotropy, as well as the temperature dependence of the scattering intensity is compatible with a simple model with the incommensurate transition temperature $T_i = 254$ K.

(III D) Simultaneous observation of the inelastic and elastic central-peak intensities. In addition to the temperature separation of 7 K between T_i and T_m , discussed in Sec. III A, these observations demonstrate a further separation of 6 K between T_m and the temperature T_e , where the intensity of the elastic central peak is a maximum. Thus, T_i and T_e differ by some 13 K. Furthermore, related measurements, carried out at much higher resolution, also demonstrated that any inelastic width to the scattering anomaly seen without the iodine cell must be less than 0.02 GHz.

A. Raman-Brillouin investigation

The initial set of experiments¹⁶ consisted of simultaneous observation of the Raman and Brillouin spectra as a function of temperature in the range 200–300 K. By collecting light from both sides of the sample, we observe simultaneously the Raman and Brillouin light scattering spectra, excited by a single-mode Ar^+ laser (Spectra-Physics 165-03) operated at 5145 Å. Viewing the spectrometer slits through the Fabry-Perot optics ensured that the same scattering volume was observed for the two sets of measurements. The Raman spectra thus provided an *in situ* probe of the temperature in the scattering volume, which eliminated any possible discrepancy between the temperature scales for the two sets of spectra. We used a Spex 1401 double grating monochromator and a pressure-scanned tandem Fabry-Perot interferometer¹⁸ to observe the Raman and Brillouin spectra, respectively. The Fabry-Perot resolution was typically 1.8 GHz, with an effective free spectral range of about 700 GHz. By using one sample with faces cut perpendicular to the crystallographic axes, we studied spectra obtained with light incident along the a (or c) axis and scattered along the c (or a) axis. With the incident and scattered light polarized along b , this is designated as $a(bb)c$ [or $c(bb)a$] geometry. A second sample was cut from a neighboring portion of the boule with faces at 45° to

the a and c axes and perpendicular to the b axis. In using it we investigated spectra with the incident and scattered light propagating at 45° to the major axes in the ac plane. The data for $\vec{q} \parallel a$ discussed below were obtained on this second crystal, with a scattering geometry as shown in Fig. 1(a). In all cases, the direction of the momentum transfer for the Raman spectra differed by 90° from that for the Fabry-Perot spectra acquired simultaneously.

An LSI-11 microcomputer controlled both the monochromator and the interferometer scans, and also accumulated and displayed both spectra simultaneously. The computer also actively controlled the tuning of the laser via a piezoelectric element controlling the tilt of the intracavity etalon. Thus it was possible to make extended runs and acquire high quality spectra at each of a number of temperatures, over a period of 80 h or more of continuous operation. A single pair of final spectra typically included multiple scans over a period of 2–8 h at a single temperature.

A molecular iodine cell rejected light scattered within 0.5 GHz of the laser frequency.¹⁹ The use of this reabsorption cell did not cause any significant distortion of the Raman spectra, which were obtained with rather wide ($\approx 5 \text{ cm}^{-1}$) slits. The numerical procedures used to correct the high-resolution spectra obtained with the tandem Fabry-Perot differed from that previously reported¹⁸ only in the use of a least squares analysis to choose the normalization parameters.²⁰ The measurements of $\Delta\nu_{LA}$ reported below, however, did not employ the iodine cell, in order to allow the most accurate determination of the LA Brillouin frequencies.

Let us first consider the Raman spectra. Certain vibrational modes which become Raman active in the low-temperature phase may be used as an intrinsic probe of temperature. For the strongest of these,

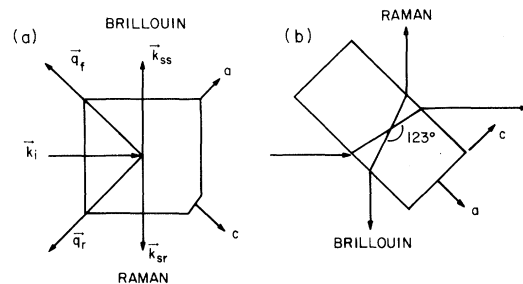


FIG. 1. (a) Scattering geometry for the sample used to obtain \vec{q} parallel to major crystal axes. The wave vector of the scattered light and momentum transfer are \vec{k}_{sf} and \vec{q}_f , respectively, for the Brillouin spectra and \vec{k}_{sr} and \vec{q}_r for the Raman. The incident wave vector is \vec{k}_i . The crystal a and c axes are as indicated. One edge of the crystal was chamfered for identification. (b) Backscattering geometry employed for study of the q dependence of the central peak.

near 150 cm^{-1} (for $\bar{q}\parallel a$), the peak position depends only weakly on temperature, but its intensity varies strongly just below $T = 154\text{ K}$. In order to extract this intensity in a quantitative fashion, we used a computer subtraction procedure, comparing the spectra in detail to one obtained well above the transition (at $T = 270\text{ K}$). If we denote a raw spectrum at a temperature T as $S(\nu, T)$, then the subtracted spectrum takes the form $S(\nu, T) - MS(\nu, 270\text{ K})$. We adjusted the multiplier M to cancel the 138 cm^{-1} component seen above the transition. Figure 2 shows the raw data [part (a)] and the result of the subtraction procedure [part (b)] for representative spectra. The ratio of the remaining peak intensity to the multiplier M then gave a reliable indicator of temperature, usable within a few K of the transition. In Fig. 3(a), which shows a typical plot of these ratios, note that a straight line drawn to fit the points extrapolates to zero within a few K of the last nonzero point available. We denote this intercept as T_R in the discussion that follows. Note that the 150 cm^{-1} peak unequivocally persists several degrees above the maximum in the central-peak intensity [Figs. 2(c) and 3(b)]. Note also that the peak movement reported by Popkov¹¹ is not observed in the subtracted spectra for $\bar{q}\parallel a$.

The importance of this probe of the actual scattering volume temperature stems from the large amount of laser heating due to absorption in our samples which were mounted with silver paste on a cold finger. Experiments in which we varied the laser power demonstrated that the laser heated the scatter-

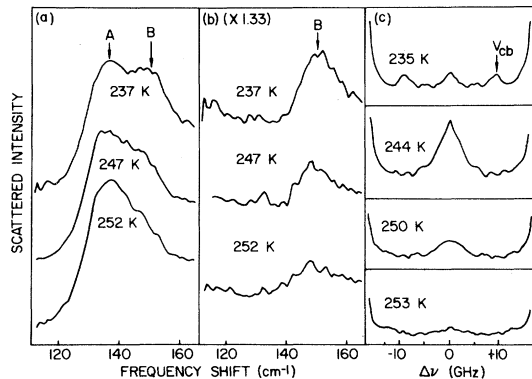


FIG. 2. Raman and Brillouin spectra taken on BaMnF_4 , illustrating the analysis used to reveal the intensity behavior of the 150 cm^{-1} peak (B). Note the clear persistence of that intensity at temperatures above that at which the inelastic central-peak intensity (with $\bar{q}\parallel c$, shown at the right) is a maximum. The wings of the LA modes are visible in the latter. Part (a) shows the raw Raman spectrum ($\bar{q}\parallel a$) over the same spectral region. A spectrum near 270 K has been subtracted to produce the results shown in part (b). Note the greatly expanded frequency scale in part (c).

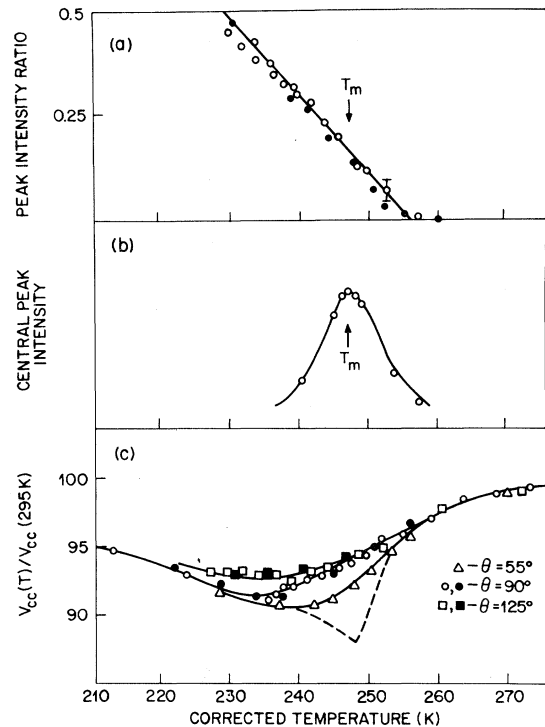


FIG. 3. Temperature dependence of three light scattering probes of the phase-transition region. Part (a) shows the behavior of the Raman intensity ratio illustrated in Fig. 2(b). Part (b) shows the central-peak intensity [see Fig. 2(c)] and part (c) shows the behavior of the acoustic velocity V_{cc} as a ratio to its room temperature value for three scattering angles θ . The dashed line shows the ultrasonic results of Fritz⁹ at low frequency.

ing volume by as much as 14 K at the power of 100 mW typically employed for the measurements reported here. All temperatures reported (here and in other sections) are corrected for such heating.

By juxtaposing the Raman data to the polarized Brillouin spectra, we find a somewhat surprising result, which is exemplified in Fig. 3(c) by the LA mode velocity determined with $\bar{q}\parallel c$. [Note that these data were obtained simultaneously with the Raman data for $\bar{q}\parallel a$, shown in Fig. 3(a).] Contrary to previous work,¹³ we find that the anomaly reported in the ultrasonic velocity by Fritz⁹ exceeds that which we observe in the frequency position of this mode near T_l . Moreover, a substantial separation exists between the temperature at which Δv_{LA} is a minimum and the temperature T_R , where the Raman ratio extrapolates to zero, as shown in Figs. 3(a) and 3(c).

Figure 4 shows the low-frequency portion of the central-peak spectra obtained with the iodine cell, which reveal a clearly inelastic component centered at

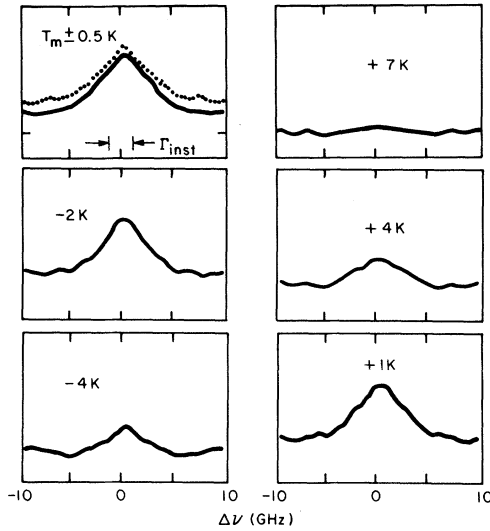


FIG. 4. Low-frequency light scattering spectra of BaMnF₄ near $T = T_m$. All temperatures are corrected for laser heating and referred to the temperature $T_m = 247 \pm \text{K}$, where the maximum intensity exists. The dotted line at upper right shows a spectrum taken at $\theta = 123^\circ$, while the remainder are for $\theta = 90^\circ$. None of the spectra is here deconvolved from the instrumental response. Note, however, that the width is substantially greater than the instrumental width, $\Gamma_{\text{inst}} \approx 2.2 \text{ GHz}$.

the laser frequency. Although its true width of $2\Gamma_{\text{CP}}/2\pi = 3.2 \pm 0.6 \text{ GHz}$ [full width at half maximum (FWHM)] is apparently insensitive to temperature, its intensity, shown in Fig. 3(b), depends strongly on temperature below T_i . The maximum in its intensity, however, occurs at a temperature T_m which is above that for which $\Delta\nu_{\text{LA}}$ is a minimum, and below T_R . The inelastic central peak was not observed in $c(bb)a$ and $a(bb)c$ geometries, and it exhibited a strongly polarized character (e.g., $I_{bb}/I_{ba} \geq 10$).

The temperature insensitivity of Γ_{CP} raises the possibility that the process responsible may not be inherently related to the phase transition. Entropy fluctuation scattering represents one such possibility. Scattering from entropy fluctuations, as from any diffusion process, exhibits a linewidth which scales as q^2 . Therefore, we measured the central-peak width for two other values of $|q|$, keeping its direction fixed. For these experiments, the light entered and left the crystal through parallel (001) or (100) faces at angles of nearly 45° . The external geometry remains a right angle one, as shown in Fig. 1(b). The refractive index determines the internal scattering angles available, which for BaMnF₄, with $n_x \approx 1.5 \pm 0.02$ for $x = a, b, c$ are $\theta = 123^\circ$ (backscattering) and $\theta = 57^\circ$ (forward scattering). The corresponding values of $|q| = (4\pi n/\lambda) \sin\theta/2$ are

3.26×10^5 and $1.62 \times 10^5 \text{ cm}^{-1}$ respectively, while the value for 90° scattering is $2.58 \times 10^5 \text{ cm}^{-1}$.

The spectra in these nonright-angle geometries provide two additional observations relative to (1) the q dependence of Γ_{CP} and (2) the dispersion of the LA velocity. First the central-peak width depends strongly on $|q|$, so much so that at $\theta = 53^\circ$ the width already approaches that of the I_2 absorption width, and we could only conclude that it did not exceed 1.6 GHz (FWHM). In the backscattering geometry, on the other hand, the peak clearly broadens, with $2\Gamma_{\text{CP}}/2\pi = 4.4 \pm 0.6 \text{ GHz}$. The formula $\Gamma_{\text{CP}} = D_t q^2$ describes these three values with $D_t = 0.14 \pm 0.02 \text{ cm}^2/\text{s}$, which, while large for a thermal diffusivity (KTaO₃ has a value of $0.056 \text{ cm}^2/\text{s}$ at room temperature,²¹ which itself is an abnormally high value), is not completely unreasonable. Thus it became very important to perform the direct measurement of the thermal diffusivity described in Sec. III B.

The dispersion in the LA velocity evident from the observations in the nonright-angle geometries appears in Fig. 3(c), where the behavior of the LA velocity, expressed as a ratio of its room temperature value, clearly depends on $|q|$. In fact, the LA Brillouin frequencies can be described qualitatively via a temperature-dependent relaxation frequency, $\Omega_R(T)$:

$$\Delta\nu_{\text{LA}} = \Delta\nu_{\text{LA}}^0 - \delta\nu \frac{1}{1 + \omega^2/\Omega_R^2}.$$

From the values observed near T_i , we conclude that Ω_R is smoothly varying and has a minimum value near T_i of order 10 GHz. Judging from the behavior of the three curves in Fig. 3(c), we conclude that this relaxation frequency Ω_R rapidly moves out beyond 1 cm^{-1} ($=30 \text{ GHz}$) as the temperature decreases below T_i . Its frequency does *not* appear to correlate with the observed behavior of the soft mode, *nor* is it consistent with $\Omega_R = \Gamma_{\text{CP}}$. Furthermore, this apparent relaxation frequency exceeds by an order of magnitude that observed by Bechtle and Scott¹³ for the TA mode $V_{cb}(\Omega_R^A \approx 0.7 \text{ GHz}$ near T_i). Its origin remains unexplained.

B. Thermal diffusivity and pyroelectricity measurements

The observed q dependence of Γ_{CP} noted above admitted an interpretation based on entropy fluctuation scattering, possibly enhanced by a coupling to the order parameter. Data on the thermal conductivity of BaMnF₄, which would allow a calculation of $D_t = \Lambda/\rho C_p$, do not exist in the literature, although Hsu²² has measured C_p . In this section we describe a direct measurement of D_t using a novel optical technique.

Achieving an accurate, nonperturbative measurement of a small temperature difference across a sample represents one of the main experimental difficul-

ties in a steady-state measurement of thermal conductivity. We employed the pyroelectric response of the sample itself as an *intrinsic* probe¹⁷ of small temperature changes to avoid such problems. While pyroelectric studies normally employ thin samples to make the thermal diffusion time short, our technique relies on working at the opposite extreme, where the thermal diffusion time dominates the experimental observations.

These experiments are discussed in detail elsewhere,¹⁷ but we shall outline the technique briefly here, since the result is of basic importance to the interpretation of our spectra. We prepared a sample as a thin elongated platelet, $1.5 \times 3 \times 6.7 \text{ mm}^3$, with the short dimension along a and the long dimension along c . One end of sample was fastened to a controlled temperature block using silver paste. A pulse of laser light absorbed on a thin metal mask at the other end caused flash heating of the free end of the sample. The pyroelectric current was then measured on three pairs of electrodes along the length of the sample as a function of time after the laser pulse. A simple model provided an accurate description of the data, as shown in Fig. 5. This model employs the one-dimensional heat-diffusion equation, assuming

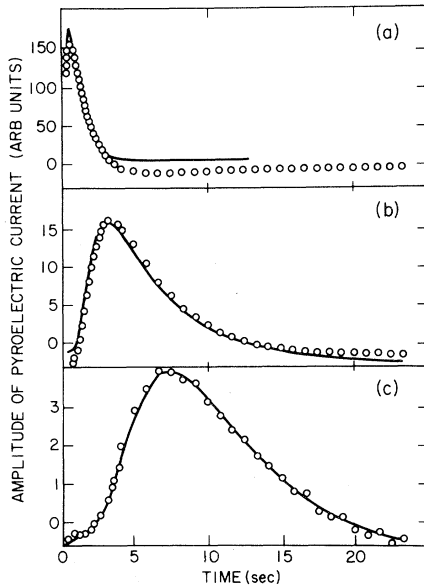


FIG. 5. Pyroelectric current observed on the three electrode pairs on a sample of BaMnF_4 prepared as described in the text, as a function of time after flash heating of one end of the sample. The solid lines represent a fit to all three profiles simultaneously, with adjustment of the thermal diffusivity. The heating pulse is 0.1 s in duration in this example, sample temperature is 185 K, and the value of $D_t = 0.0062 \text{ cm}^2/\text{s}$ results from the fit shown. The theoretical curves in (a) and (c) are multiplied by factors of ~ 0.8 and ~ 1.1 , respectively, to account for variation in electrode size.

conductive heat transfer only, and no boundary resistance where the crystal was attached to the block. The straightforward Fourier series solution of this model yields the solid lines shown in the figure, where we have fit all three curves by varying the value of D_t (in principle, each curve provides an independent measurement so this is a check of internal consistency). In the calculation we use the known positions and spatial extents of the electrodes, but we ignore fringing effects, which should cancel to first order. The zero offset visible there is due to dc offset in the electronics. As a result of the analysis illustrated in Fig. 5, we extract a value for D_t related to heat diffusion along the c axis.

The essential conclusion is that the numerical value of $D_t = 0.14 \text{ cm}^2/\text{s}$ extracted from the spectra (Sec. III A) far exceeds the values of the thermal diffusivity ($\sim 0.005 \text{ cm}^2/\text{s}$) near T_i . The dominant systematic errors are those due to radiative heat losses, conduction through the electrodes, and possible errors due to anisotropy in Λ and misalignment of the crystal. We note that these errors could only serve to increase the observed value. Thus, since the value of $0.005 \text{ cm}^2/\text{s}$ probably represents an upper limit, we conclude unequivocally that entropy fluctuations do *not* cause the observed inelastic central peak.

As a byproduct of these measurements, the amplitude factors in the fits yield a sensitive measurement of the pyroelectric response near the phase transition. The pyroelectric coefficient crosses zero in this region of temperature,⁴ corresponding to a peak in the spontaneous polarization, while the slope appears to change¹⁷ by a factor of about 1.7. The source of both the zero crossing and the slope change remain unknown, but this observation lends credence to the idea that the zero crossing at $T \approx 254 \text{ K}$ represents an actual transition temperature.

C. Phason anisotropy

Having eliminated entropy fluctuations as the cause of the observed inelastic central peak, we now consider the possible mechanism of phason scattering. We have already shown in Sec. II that the phason in BaMnF_4 has the proper symmetry to scatter light.

Bhatt and McMillan^{23,24} have developed a dynamical Landau theory for the case of a charge-density wave transition applicable to the layered transition-metal dichalcogenides.²⁵ They consider the high-temperature phase (i.e., no static distortion), including a coupling of a relaxing order parameter to a single optic phonon. They obtain the dynamic structure factor and dispersion of the soft-mode branch in the vicinity of \bar{k}_0 . The characteristic relaxation time of the overdamped incommensurate excitation is found to be

$$\tau_q = \frac{\gamma}{2} [a'(T - T_i) + e(\bar{q} \cdot \bar{k}_0)^2 + f|\bar{q} \times \bar{k}_0|^2]^{-1}, \quad (4)$$

using our notation where \vec{k}_0 is the incommensurate wave vector, and the wave vector of the excitation is $\vec{k} = \vec{k}_0 + \vec{q}$. The constants a' , e , and f are the coefficients of the quadratic terms in the free-energy expansion in powers of the order parameter, and determine, respectively, the temperature and wave-vector dispersion of the excitation above T_i in the neighborhood of the incommensurate wave vector, \vec{k}_0 . (Our a' is one-half that used previously,²³ to be in accordance with existing work on BaMnF₄.)

This model is not directly applicable to the case of BaMnF₄ for two reasons. First, the incommensurate wave vector in BaMnF₄ lies at the zone boundary, and therefore has a star of four components. Second, the model as stated²³ applies only above the transition, in the normal phase. In what follows then, we cannot use the model of Bhatt and McMullan directly. However, this model can be used to describe the phason anisotropy in BaMnF₄, as done previously,⁷ by making two assumptions. Firstly, since phason dynamics should be relatively insensitive to temperature below T_i , we may use the expression (4) evaluated at T_i to describe the phason dispersion just below T_i . We note in passing that other (amplitudelike) modes behave as normal soft modes below T_i , and are strongly temperature dependent. Secondly, in order to handle the fact that \vec{k}_0 lies at the zone boundary, let us consider why there is an anisotropy in the first place (in this or any other model). The reason is basically that there exists a direction in which the incommensurate distortion can "slide" with respect to the ambient lattice with no cost in energy. Clearly, the phason dynamics for a modulation of the phase along that direction (a fluctuation in the period of the incommensurate wave vector) may be fundamentally different than for modulation of the phase perpendicular to that direction (a fluctuation in the direction of the incommensurate wave vector). Hence there is anisotropy in the phason dispersion curve. However, in a material such as BaMnF₄, the special direction is not parallel to \vec{k}_0 , which has two commensurate components, but rather lies along the a axis. That is, we must replace \vec{k}_0 in (4) above by its *incommensurate component*.

We shall now provide a theoretical basis for these conjectures. The generalization to temperatures below T_i , but close to it, is readily done by expanding the free energy for a single incommensurate CDW (or distortion) Φ at a wave vector \vec{k}_0 :

$$F(\Phi) = \int d\vec{r} [a'(T - T_i)|\Phi|^2 + b|\Phi|^4 + e|(\vec{k}_0 \cdot \vec{\nabla} - k_0^2)\Phi|^2 + f|\vec{k}_0 \times \vec{\nabla}\Phi|^2] \quad (5)$$

about its equilibrium value. First, we remove the rapid dependence due to the wave vector \vec{k}_0 :

$$\Phi = \phi e^{i\vec{k}_0 \cdot \vec{r}} \quad (6)$$

to obtain F in terms of the slowly varying $\phi(r)$

$$F\{\phi\} = \int d\vec{r} [a'(T - T_i)|\phi|^2 + b|\phi|^4 + c_{\parallel}|\nabla_{\parallel}\phi|^2 + c_{\perp}|\nabla_{\perp}\phi|^2] \quad (7)$$

where $c_{\parallel} = ek_0^2$, $c_{\perp} = fk_0^2$, and ∇_{\parallel} and ∇_{\perp} are gradients in the direction parallel to and in the plane perpendicular to \vec{k}_0 . Expanding ϕ about its equilibrium value, $\phi_0 = [a'(T_i - T)/2b]^{1/2}$:

$$\phi = \phi_0 [1 + (\delta A + i\delta\psi)e^{i\vec{q} \cdot \vec{r}}] \quad (8)$$

where $\phi_0\delta A$ and $\phi_0\delta\psi$ represent the (real) amplitudes of the amplitude and phase mode (phason) of the order parameter, respectively, with a wave vector $\vec{k} = \vec{k}_0 + \vec{q}$ near the incommensurate wave vector \vec{k}_0 , we obtain, to quadratic order in the amplitudes

$$\frac{F - F_{\text{eq}}}{\Omega} = [2a'(T_i - T) + c_{\parallel}q_{\parallel}^2 + c_{\perp}q_{\perp}^2](\phi_0\delta A)^2 + (c_{\parallel}q_{\parallel}^2 + c_{\perp}q_{\perp}^2)(\phi_0\delta\psi)^2 \quad (9)$$

where $F_{\text{eq}} = F\{\phi_0\}$ is the equilibrium free energy. The extension of the previous result²³ then, for the phason relaxation time below T_i , is given by

$$\tau_q^{\text{phason}} = \frac{1}{2} \gamma / (c_{\parallel}q_{\parallel}^2 + c_{\perp}q_{\perp}^2) \quad (10)$$

while the characteristic frequency (relaxation time) for an underdamped (overdamped) amplitude mode would have a temperature-dependent term $2a'(T_i - T)$ in addition to the gradient (q^2) contributions.

In BaMnF₄ there are four equivalent wave vectors in the star of \vec{q}_0 , which describe the primary order parameters¹⁶

$$\vec{q}_1 = (0.39, +0.5, +0.5), \quad \vec{q}_2 = -\vec{q}_1 \quad ,$$

$$\vec{q}_3 = (0.39, -0.5, +0.5), \quad \vec{q}_4 = -\vec{q}_3 \quad .$$

Denoting by Q_i the amplitude of the order parameter with wave vector \vec{q}_i , the free energy, generalized to include the gradient terms as per Eq. (7) is (using the notation of Cox *et al.*¹⁴)

$$F = \int d\vec{r} \left\{ a(Q_1Q_2 + Q_3Q_4) + \sum_{\mu} c_{\mu} (\nabla_{\mu}Q_1\nabla_{\mu}Q_2 + \nabla_{\mu}Q_3\nabla_{\mu}Q_4) + V_1(Q_1^2Q_2^2 + Q_3^2Q_4^2) + V_2Q_1Q_2Q_3Q_4 + Ve^{i\alpha}Q_1^2Q_4^2 + Ve^{-i\alpha}Q_2^2Q_3^2 \right\} \quad (11)$$

where $a = a'(T - T_i)$, c_{μ} , V , V_1 , V_2 , and α are real. The sum on μ is over the three axes set by the incommensurate component of \vec{q}_i , i.e., parallel axis along a and two in the plane normal to it. We retain only the anisotropy between the a axis (c_{\parallel}) and the bc plane (c_{\perp}), as is verified experimentally in the

present work (this and Sec. III D).

The requirement of atomic displacements being real implies

$$Q_1 = Q_2^* = \phi_1 e^{i\psi_1}, \quad Q_3 = Q_4^* = \phi_2 e^{i\psi_2},$$

where ϕ_i and ψ_i are real. In terms of the new variables,

$$F = \int d\vec{r} \left[\sum_{i=1}^2 \{ a \phi_i^2 + c_{\parallel} [(\nabla_{\parallel} \phi_i)^2 + \phi_i^2 (\nabla_{\parallel} \psi_i)^2] + c_{\perp} [(\nabla_{\perp} \phi_i)^2 + \phi_i^2 (\nabla_{\perp} \psi_i)^2] + V \psi_i^4 \} + [V_2 + 2V \cos(\alpha + 2\psi_1 - 2\psi_2)] \phi_1^2 \phi_2^2 \right]. \quad (12)$$

As shown by Cox *et al.*,¹⁴ depending on the relative values of the quartic coefficients, two static solutions are possible below T_i

$$(i) \quad \phi_1^0 = \phi_2^0 = a'(T_i - T)/(2V_1 + V_2 - 2V) \\ \text{for } 0 < 2V_1 + V_2 - 2V < 4V_1$$

and

$$(ii) \quad \phi_1^0 = a'(T_i - T)/2V_1, \quad \phi_2^0 = 0 \\ \text{for } 0 < 4V_1 < 2V_1 + V_2 - 2V.$$

The relative phases are given by $2(\psi_1^0 - \psi_2^0) = \pi - \alpha$. We consider case (i) first. Expanding the order parameters around the static value

$$\phi_i = \phi_0(1 + \delta A_i) \exp(i(\psi_i^0 + \delta \psi_i)), \quad (13)$$

where $\delta A_i, \delta \psi_i \sim \cos(\vec{q} \cdot \vec{r})$, and keeping up to quadratic terms in the displacements δA_i and $\delta \psi_i$, we obtain

$$\frac{2(F - F_0)}{\Omega} = 4V_1 \phi_0^4 (\delta A_1^2 + \delta A_2^2) + 4(V_2 - 2V) \phi_0^4 \delta A_1 \delta A_2 + 4V \phi_0^4 (\delta \psi_1 - \delta \psi_2)^2 \\ + (c_{\parallel} q_{\parallel}^2 + c_{\perp} q_{\perp}^2) \phi_0^2 (\delta A_1^2 + \delta A_2^2 + \delta \psi_1^2 + \delta \psi_2^2). \quad (14)$$

This leads to four modes, one of which, corresponding to in-phase oscillations of the phases ($\delta \psi_1 = \delta \psi_2$), can be identified as the phason (Goldstone boson for $q = 0$) with a temperature-independent relaxation time (following the analysis of Bhatt and McMillan^{23,24}):

$$\tau_q^{\text{phason}} \sim (c_{\parallel} q_{\parallel}^2 + c_{\perp} q_{\perp}^2)^{-1}. \quad (15)$$

We can repeat the analysis above for case (ii), in which case the phason is simply the phase oscillations $\delta \psi_1$ of the nonzero order parameter, and we obtain exactly the same result (15) for the corresponding phason relaxation time. Thus, in either case, the phason relaxation rate is given by

$$\Gamma_p \equiv \frac{1}{\tau_q^{\text{phason}}} = D_{\parallel} q_{\parallel}^2 + D_{\perp} q_{\perp}^2 \\ = q^2 (D_{\parallel} \cos^2 \phi_q + D_{\perp} \sin^2 \phi_q), \quad (16)$$

as used previously,⁷ where ϕ_q is the angle \vec{q} makes with the incommensurate a axis. For anisotropic Landau parameters (c_{\parallel} and c_{\perp}), Eq. (16) would lead to an equivalent anisotropy in Γ_p . Thus we see that by applying the model of Ref. 22 to the free energy

appropriate to BaMnF_4 ,¹⁴ we obtain the simplest form one could expect such an anisotropy to assume.

Indeed, attempts to measure the central-peak width in geometries with $\vec{q} \parallel a$ and with \vec{q} at 45° between a and c had been unsuccessful due to lack of signal. Since there is some scattering from other processes in this region, and also since the mode may be coupled to the acoustic phonons, it would become difficult to distinguish the central peak from a flat background if its width increased above 15 GHz while its integrated intensity remained constant. With this in mind, we investigated the spectrum obtained in the region of angle accessible by rotating the crystal used for the $\vec{q} \parallel c$ measurements, correcting for refraction at the faces. Figure 6 shows two of the resulting spectra, which do indeed exhibit the anticipated anisotropy. Figure 7 shows the true spectral widths (FWHM, deconvolved), along with a curve which represents a fit of Eq. (16) to the five points at which the feature was clearly observed. The parameters resulting from the fit have the values $D_{\parallel} = 0.98 \text{ cm}^2/\text{s}$ and $D_{\perp} = 0.14 \text{ cm}^2/\text{s}$, which correspond to a large anisotropy of $D_{\parallel}/D_{\perp} = 6.8$. As is evident in the figure, this anisotropy is qualitatively consistent with the failure to observe the feature at the two orientations indicated with the arrows.

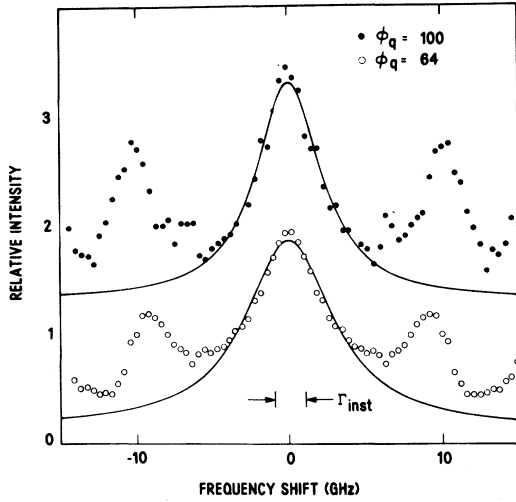


FIG. 6. Central-peak spectra taken for two off-axis orientations of \vec{q} . The angle ϕ_q is that between \vec{q} and the a axis in the ac plane. The lines are Lorentzians drawn to fit the central peak. The features visible at $\sim \pm 10$ GHz are the TA mode, visible more strongly in these off-axis geometries. The strong LA modes are outside the spectral region displayed. The instrumental resolution is $\Gamma_{\text{inst}} = 1.9$ GHz.

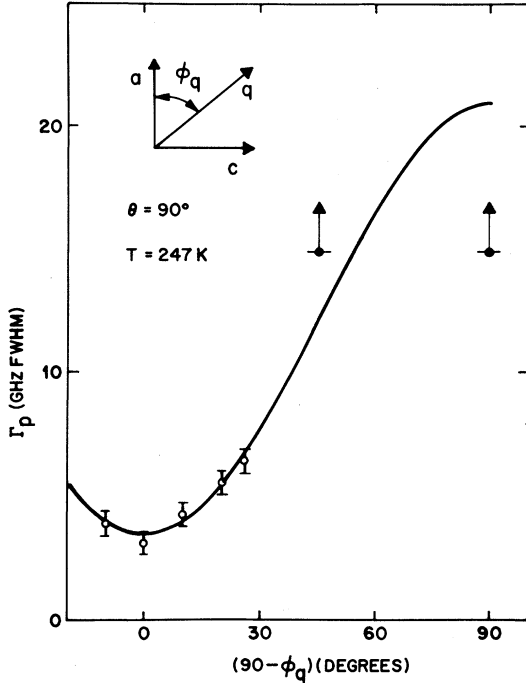


FIG. 7. True linewidth (full width at half maximum) of the inelastic central peak (Γ_p) as a function of ϕ_q in the ac plane. The temperature and scattering angle are held constant at 247 K and 90° , respectively. The points at $\phi_q = 45^\circ$ and 90° represent negative observations, from which minimum values of Γ_p may be inferred under appropriate assumptions (see text). The line represents a calculation using $D_{\parallel} = 0.98$ cm²/s and $D_{\perp} = 0.14$ cm²/s in Eq. (16).

Other possible explanations of an inelastic central peak with a strongly q -dependent linewidth may exist. Nevertheless, the experimental observation of the maximum in the scattering intensity near T_i and the high degree of anisotropy lend support to our view that the scattering arises directly from the phason mode.²⁶ Using these values of $D_{\parallel, \perp}$ the values of Γ_q at a reduced wave vector of 0.1 are of the order of 10–100 meV, which is consistent with the observation in neutron scattering that the incommensurate excitation above T_i becomes underdamped at wave vectors in this range. The expression for the underdamped incommensurate excitation frequency above T_i is a form similar to that given previously²³:

$$\omega_q^2 = \omega_{q0}^2 / (1 + \beta \omega_{q0} \tau_q) ,$$

where ω_{q0} is the frequency far from the transition and β is a coupling parameter. (Note that this is a more accurate expression for ω_q than the approximation given in Sec. V of Ref. 22.) However, using this expression with q -independent ω_{q0} and β , we find that the anisotropy in the q dependence of the incommensurate excitation above T_i observed in the neutron scattering experiment¹⁴ is precisely the reverse of that predicted using the value of $D_{\parallel}/D_{\perp} = 6.8$ obtained here. That is, the slope of the dispersion for $\vec{q} = (\xi, 0.5, 0.5)$ is expected to be greater than that for $\vec{q} = (0.39, \eta, \eta)$ by a factor of $2.6 = \sqrt{6.8}$, while the observed ratio is about 0.6. This discrepancy may stem from the relatively large values of \vec{q} involved in the neutron scattering experiment, requiring inclusion of higher-order terms in the gradient expansion of the free energy, and possible q dependence of the value of ω_{q0} . The latter possibility is indicated by the temperature-insensitive dispersion curve observed in neutron scattering.¹⁴ In either case, we note that the anisotropy we observe ($D_{\parallel} > D_{\perp}$) is for the limit of small q where the Landau expansion is expected to hold and is, further, consistent with the plausibility arguments given by Boriack and Overhauser.²⁶

D. Elastic scattering

As mentioned above, the phason light scattering activity is dependent on the presence of a static distortion. Since the phason frequency does not vary strongly below T_i , we expect its intensity (within mean-field theory) to scale as the square of the order parameter $I_{\text{CP}} \propto \psi_0^2$, for temperatures near T_i . Thus, on the basis of our interpretation, we have to assume that the temperature where the maximum central-peak intensity occurs, T_m , is significantly below T_i , since the central-peak intensity extrapolates to zero at $T \sim T_m + 7$ K. The behavior of the Raman intensity ratios described in Sec. III A suggests the same relationship. As a further check of this condition, we carried out one additional experiment. Using a fresh

sample from the same boule, selected for highest possible optical quality, we attempted to observe the anomaly in the elastic scattering reported by Lockwood.¹³

Lacking evidence to the contrary, we initially assumed that the rather sharp peak in the elastic intensity at $T = T_e$ reported by Bechtle *et al.*¹³ represented an accurate measurement of the transition temperature, i.e., that $T_e = T_i$. Therefore, based on the results discussed thus far, we would expect $T_e \sim T_m + 7$ K. We performed experiments to check this assumption and also to search for a finite width in the peak seen without the iodine cell. In the attempt to resolve the peak width we used a Burleigh triple-pass interferometer, operated at high resolution, $\Gamma_{\text{inst}} = 0.25$ GHz. The crystal quality was such that the integrated intensity in the elastic peak was only larger than the LA phonon (with $\vec{q} \parallel a$) by a factor of 14 at room temperature. The elastic peak was of course instrumentally narrow, while the LA peaks showed a real full width of 1.05 GHz, or $\sim 5\%$, most of which was kinematic, due to the large ($f/3.5$) solid angle of collection.

The anomaly in the elastically scattered intensity in $b(aa)c$ geometry (as used by Lockwood) occurred at a surprisingly low temperature (see below) and constituted an increase by a factor of nearly 2 above a background. Except for this background which exhibited a gradual minimum near 255 K, the shape of the intensity anomaly on heating through T_e closely resembled that reported by Lockwood.¹³ On cooling, the more gradual increase observed on approaching T_e from above (see Fig. 8) continued as T_e was traversed, even by as much as 10 K. On one occasion, the temperature was controlled for 12 h after careful cooling to $T = T_e - 5$ K with no noticeable change in this intensity. Only when the crystal was cooled (to ~ 220 K) and heated towards T_e did we observe the behavior reported by Lockwood and shown in Fig. 8. Both cooling and heating curves were reproducible on multiple runs in different regions of the sample. It should be noted, however, that the scattering volume was always chosen for low elastic scattering above and below the transition. The integrated intensity in the anomaly at T_e on heating was 10–20 \times that contained in the LA peak.

In the vicinity of T_e , careful measurement of the peak width on heating showed no broadening of the instrumental response outside an experimental error of 0.02 GHz. A width of 0.7 GHz ($\sim 3\Gamma_{\text{inst}}$), as predicted by the analysis of Bechtle *et al.*,¹³ would have been easily observed.

As mentioned above, the anomaly in the elastic scattering intensity occurred at an unexpectedly low temperature, namely 241 K. In view of the large amount of sample heating present, and the fact that we used a different temperature sensor, it seemed important to check this result. To do so, we em-

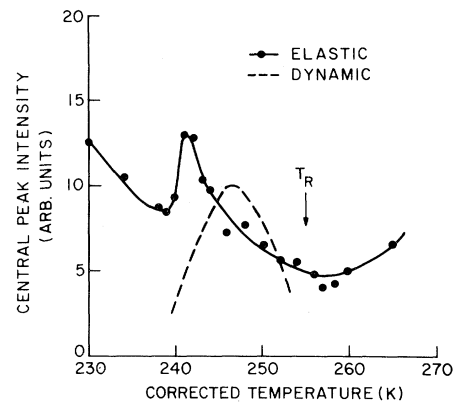


FIG. 8. Dynamic (dashed line) and elastic (dots, solid line) central-peak scattering intensity as functions of temperature below T_i , taken on the same apparatus alternately with and without the iodine cell. The temperature T_R is the transition temperature inferred from Fig. 3(a).

ployed the tandem Fabry-Perot used for the inelastic central-peak measurements (Sec. III A). By simply removing or inserting the iodine cell we could then observe the elastic or inelastic component of the peak (the former being stronger by about 10^3).

Figure 8 shows the results, where we plot both the light intensity observed without the iodine cell at the laser frequency and the inelastic central-peak intensity observed with the iodine cell, taken on the same experimental run. The scattering geometry of $b(aa)c$ coincided with that employed by Lockwood.¹³ The inelastic central peak in this geometry is somewhat weaker (30–40%) but otherwise identical to that observed with $\vec{q} \parallel c$, providing further substantiation of the model represented by Eq. (16). The temperatures T_m and T_e , where the two intensities are maximal, exhibit a clear separation, but in a direction opposite that which might be expected, namely $T_m - T_e \sim 6$ K. Since the two sets of spectra were observed on the same run, this temperature separation cannot be an experimental artifact. We consider a possible explanation of this behavior in Sec. IV.

IV. DISCUSSION

The main questions that remain, then, involve the value of the actual transition temperature and the explanation of the variations in the intensity of the elastically scattered light. We shall also consider the interpretations of other workers^{13,15} in relation to that proposed here.

To begin with, we summarize in Table I the temperatures at which the various anomalies occur. We note that all the measurements in the lower portion of the table relate to neighboring pieces cut from the

same boule. The different values shown in the upper portion could be attributed to sample differences, rather than to differences in the experimental probe. However, such an objection is not relevant to comparisons among the measurements reported in this paper, since we utilized simultaneous measurement to maintain correspondence among the various sets of temperature measurements shown. Clearly, these various indicators must bear different relationships to the incommensurate transition temperature, and could, in fact, indicate the presence of more than one transition. We cannot exclude the latter possibility.²⁷ In fact, we have no completely definitive indicator of T_i . This situation is perhaps not surprising for so subtle a transition. For example, the relationship between T_i and the behavior of dP_s/dT remains unclear at this time, even though the zero crossing does occur very near T_R . Moreover, although the intensity of the Raman band at 150 cm^{-1} provides a clear extrapolation to $T_R \sim 254\text{ K}$, the intensity could be influenced by the presence of large critical fluctuations¹⁴ and, of course, depends on the temperature independence of the profile being subtracted in Fig. 2. The other modes appearing below T_i are sufficiently weak near T_i as to prevent any reliable consistency checks using other modes. The only other relevant indicator is the central-peak scattering itself, which peaks at 247 K , but also extrapolates to the background level near 254 K . It also exhibits a strong dependence on the magnitude as well as the direction of \vec{q} but is substantially T independent over the entire range where the width is readily measurable. This body of evidence must be considered in light of two limiting possibilities: $T_i \approx T_m$ or $T_i \approx T_R$.

Let us consider the first case. If we identify

$T_i \approx T_m$, then there is a natural explanation for the peak in I_{CP} at T_m . However, it cannot be a process with scattering allowed in first order in the normal phase. Hence, the intensity for $T_m < T < T_R$ must be due to higher order scattering. However, this is inconsistent with the strong q dependence of Γ for $T > T_m$. Moreover, if the Raman intensity above T_m were due to fluctuations one would certainly expect at least a break in that curve near T_m , not a straight line.

On the other hand, the identification $T_i \approx T_R$ appears consistent with all the data. In this case, the morphically induced cross section for phason scattering would grow from zero below T_R , as observed (Fig. 3) between T_m and T_R . Also, the observed behavior of the Raman intensity is then explained automatically and the T independence of Γ is consistent with the expected phason behavior. Moreover, this identification provides a possible explanation for the peak in P_s , although the reason for that relationship must remain unclear until the structure is known in detail. As we shall see below, based on this interpretation we may attribute the scattering mechanism to the coupling of the phason to the LA phonon. Thus the peak in intensity at T_m could be either the result of a temperature variation in that coupling or the result of a second phase transition.²⁷

We conclude, therefore, that the weight of the evidence favors the interpretation that $T_i \approx T_R$. In what follows when we use the notation T_i , we refer to this identification. It should be noted that we have considered only two limiting cases here. Some intermediate value of T_i near T_R would also be consistent with the above arguments, and would not alter the discussion below.

The behavior of the elastic scattered intensity correlates with $p \equiv dP_s/dT$, with the zero crossing of p falling at or very near T_i . In the data of Glass *et al.*,⁴ a peak in $p(T)$ is present roughly 15 K below the zero crossing. It seems possible that the relative value of p represents a measure of the sensitivity of the structure of perturbations other than temperature (such as certain defects, etc., which may locally alter T_i). In this case, the scattering from static defects of this sort would contain a term proportional to $[p(T)]^2$. The near correspondence between the peak in the elastic scattering intensity and the peak in $p = dP_s/dT$ may thus be more than coincidence. However, the value of T_e may not be a reliable indicator of a transition, particularly given the apparent hysteresis in its behavior of warming and cooling, which suggests a possible domain effect.

The order-parameter symmetry in BaMnF_4 actually requires the existence of four equivalent order parameters, with different wave vectors. These modes combine linearly into four normal modes, only one of which is the Goldstone mode,²⁸ having zero frequency at $\vec{k} = \vec{k}_0$. In the above discussion we

TABLE I. Various transition indicators in BaMnF_4 .

Experiment	Indicated temperature (K)
Other work	
Ultrasonic (Ref. 9)	247
Raman (Refs. 10 and 11)	255
Pyroelectric (Ref. 4)	255
Present work	
Raman (T_R)	254 ± 1
Dynamic central peak	
Maximum (T_m)	247 ± 1
Disappearance	254 ± 1
Pyroelectricity dP_s/dT	
Zero crossing	255 ± 2
Maximum	241 ± 1
Elastic central peak (T_e)	241 ± 1

have assumed that the other three modes lie outside the frequency range relevant to the central-peak spectra. Barring an accidental cancellation of large parameters, this assumption should be valid.

Our interpretation of the spectra differs from that given by Lockwood *et al.*¹⁷ We have reproduced one of their spectra in Fig. 9. The fit that results from their model contains four components: the (elastic) central mode, the TA mode, and two overlapping propagating modes to describe the asymmetric LA phonon peak. The central component is instrumentally narrow and the weak TA mode is insensitive to temperature. Of the two modes used to describe the asymmetric LA peak, the one lower in frequency is identified as the phason, in direct conflict with our interpretation based on an overdamped phason mode.

Let us now consider whether it is possible to reconcile the data of Lockwood *et al.*¹⁵ with our interpretation. There is an obvious approach to use, namely, we can assume that the LA phonon is coupled to the overdamped phason which we have observed. In fact, there is reason to believe²⁹ that *all* the phason scattering intensity may stem from its coupling to the acoustic mode. If we make the assumption that this is the case, we can then fix the coupling constant using the intensity ratio between the central peak and the LA phonon. That ratio is not known with precision, but reaches a maximum of about 15% (in integrated intensity). Using this value, along with the extrapolated value of the width from Fig. 7 for the

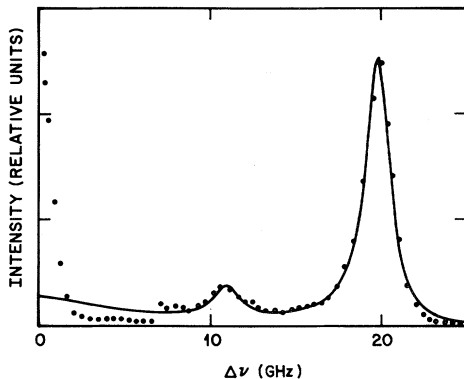


FIG. 9. Comparison of the calculated LA spectral profile with that observed by Lockwood *et al.* (Ref. 15). The dots represent the observed profile (with a gain change of $20\times$ at the laser, due to elastic scattering contamination of their spectrum) and the solid line represents the calculation based on coupling of the quasiharmonic LA mode with an overdamped phason mode using the width taken from the extrapolated curve in Fig. 7. A small contribution from the TA mode active in this geometry is included simply as a superposition of a quasiharmonic peak in order to more closely describe the observed spectrum. The overall intensity of the calculated spectrum has been adjusted to agree with that observed.

geometry employed by Lockwood *et al.*¹⁵ we obtain a *parameter free* fit to the LA lineshape which is compared to the reported spectral profile in Fig. 9. Clearly, this model provides a fit to the LA profile of quality equivalent to that obtained by Lockwood *et al.*¹⁵ and with three fewer parameters. Moreover, it describes the central peak reported here, as well. The extra mode reported in Ref. 13 is an artifact of the fitting procedure, and will have an apparent intensity proportional to the coupling constant. Naturally, it is possible to decompose our calculated LA line shape in the same manner as in Ref. 13, with the same results, but we find that parametrization less useful and, in fact, misleading.

It must also be noted that the weak central peak observed here, and shown in the calculated line in Fig. 9 would have been obscured in their spectra by the tail of the elastically scattered light which is some $600\times$ stronger at its peak. Of course, their model cannot reproduce that overdamped component which, as shown by the above analysis, is responsible for the LA asymmetry. Lockwood *et al.* have fit their spectra using a detailed response function, concluding that no excess scattering is present below ~ 10 GHz. However, it is highly questionable whether it is possible to know the instrument response function in the requisite detail, especially in view of the fact that the same data were used previously¹³ to demonstrate the presence of a singular dynamic central peak. That interpretation has of course been retracted in the latest version,¹⁵ but the fact remains that it is highly difficult to use an unassisted single-pass Fabry-Perot interferometer to study weak, broad features in close proximity to strong narrow ones. By the use of the iodine-cell technique, we have eliminated this problem in the present work, and have demonstrated that the dominant new scattering at low frequencies below T_i lies in a diffusive central peak.

The presence of the TA mode does not change the above analysis in any way: it has been added to the calculation by a simple superposition. The accuracy of the data in Ref. 13 is insufficient to allow a decision as to whether there is a corresponding asymmetry in it as well, as might result from coupling of the phason and the TA mode. Our model thus contrasts with that used by Bechtle *et al.*¹³ but that difference is mainly due to the frequency range involved. They considered a model based on coupling between the TA mode and the phason. They noted that pair-wise couplings involving these modes and the amplitude mode, although allowed, were apparently unimportant. Since the LA dispersion is not important in the same region of \bar{q} , they ignored any role of the LA phonon. Thus, they reduced the four-mode system to a more tractable two-mode problem. Since the TA mode scattering is weak and predominantly depolarized, this TA-phason coupling predicts a weak depolarized central peak. That such a

peak has never been observed may simply be a consequence of weak scattering strength. Even at very low q , where the observed dispersion is maximal, its integrated intensity would be only $\sim 20\%$ of that of the TA mode. At higher q , as in our experiments, it would be negligible, especially in contrast to the contribution from the LA coupling, since the LA dispersion becomes evident in just this range of q and the LA intensity is largely polarized and considerably stronger.

However, a point of conflict does exist between their interpretation and ours. They assume that the coupling is q independent, and thus attribute the observed dispersion to a finite relaxation frequency for phasons at $q=0$. This is a most unusual behavior, at least for the pure system. The model of Bhatt and McMillan²³ predicts $\Gamma_p \propto q^2$, while the work of Boriack and Overhauser²⁶ suggests that $\Gamma_p \sim q$ in the overdamped regime. In either case we conclude that $\Gamma_p \ll \omega_{TA}$ for all $\vec{q} \parallel c$ accessible in light scattering: the two frequencies could cross only at higher \vec{q} . Extrapolating our measured values of Γ_p to the values of \vec{q} employed in the TA dispersion measurements, we predict a phason width on the order of 0.02 GHz, in contrast to the apparent relaxation frequency of $\Gamma_r \sim 0.7$ GHz reported.¹³

To clear up this discrepancy, we begin by noting that their model does not in fact hinge on the assumption that the relaxation process involved is a single phason. Therefore, we propose that the process responsible for the TA dispersion may be a two-phason process (analogous to phonon-density fluctuations in normal crystals) involving coupling to two modes on the phason branch at \vec{k} and $\vec{k} \pm \vec{q}$. Such a process would have a finite frequency width for $|\vec{q}| \rightarrow 0$. If the coupling is independent of q , then the relevant phason pairs must be restricted to low values of $|\vec{k} - \vec{k}_0|$ (e.g., by matrix element effects) in order to explain the low value of Γ_r . However, it may also be that the value of Γ_r is only an apparent value stemming from a q dependence of the coupling constant, and, in fact, does not represent a true characteristic frequency of the two-phason process involved. That is, it may be that the coupling of the phasons to the TA mode increases sharply for $|\vec{q}| \leq 10^4 \text{ cm}^{-1}$. (If a similar q dependence occurs for the LA mode, the characteristic $|\vec{q}|$ must be $\sim 10^5 \text{ cm}^{-1}$.) We would hope that a complete model for the interaction of the acoustic modes with the phason will eventually provide a consistent interpretation of all these results.

The fact that the intensity of the inelastic central peak has a maximum at 247 K and dies away at lower T may relate either to the scattering mechanism or to the presence of another phase transition. Within the framework of the model above, where the LA-phason coupling constant would grow roughly as $|\psi_0|^2$ below $T_i = 254$ K, it seems more probable that the maximum is related to a second phase transition. In

the accompanying paper, Scott *et al.* present specific-heat evidence for a second phase transition. The temperature at which the central-peak intensity is a maximum ($T_m = 247$ K) coincides closely with the lower phase transition they observe.

Based on yet-unpublished x-ray data, Scott *et al.*²⁷ suggest that the lower phase transition may actually represent lock-in. We note that such an interpretation might explain the disappearance of phason scattering below 247 K. However, the neutron scattering experiments of Cox *et al.*,¹⁴ carried out on samples from the same source as ours, clearly show \vec{k}_0 to be incommensurate. Thus, we doubt that the lock-in interpretation is correct. We would suggest, on the contrary, that a model recently proposed for BaMnF₄ by Natterman and Przystawa³⁰ may be applicable. They find that, within a Landau model explicitly including umklapp terms in the free energy, there may be a narrow temperature range where \vec{k}_0 lies in the ab plane. The second phase transition then represents a partial lock-in to an incommensurate structure which remains incommensurate along a only. The applicability of such a model has been controversial³⁰ and must remain speculative at this time, but we note a recent independent report by Toledano³¹ that such a structure is allowed by symmetry in the case of BaMnF₄. Also, such a sequence of phase transitions has been reported for the case of biphenyl.⁸

A second possibility is that a phase transition may occur between the two structures discussed by Cox *et al.*¹⁴ If the lower temperature phase is that for which $A \neq B$ (in their notation), then it could account for domains which might exist below T_m and might be responsible for the anomalous elastic intensity at T_e . It would seem that such a transition must be first order.

Clearly, much work remains to understand fully the transition to the incommensurate phase in BaMnF₄. We have presented here an analysis of central-peak spectra, Brillouin spectra, Raman spectra, thermal diffusivity, and elastic scattering. On this basis we have suggested a new and consistent interpretation of existing data, particularly with regard to the transition temperature, and have identified the polarized dynamic central peak as due to phason scattering mediated by the acoustic-phason interaction. This interpretation requires identification of the incommensurate transition temperature as $T_i = 254 \pm 1$ K for our samples, which lies 7 K above T_m and 13 K above T_e , but which coincides with T_R and with the zero crossing of the pyroelectric coefficient. We have shown that, within the context of the model developed previously²³ for $T > T_i$, the phason is expected to have a relatively temperature-independent relaxation time below T_i and that the main anisotropy should exist between the directions parallel and perpendicular to the direction of incom-

mensuration. Both these predictions are borne out by our experimental results. Previous neutron scattering data¹⁴ indicate the presence of an anisotropy reversed in sign at much higher \bar{q} , suggesting the role of other q dependences not included in our model. We have also shown that any inelastic width to the scattering anomaly visible without the iodine cell must be less than 0.02 GHz. Finally, we have shown that a simple model assuming coupling of the phason to the LA mode reproduces the details of the asymmetric LA lineshape recently reported by Lockwood *et al.*, although our interpretation of those spectra differs from theirs. Remaining questions center on the explanation of the behavior of $p = dP_s/dT$ near T_i , its relationship to the elastic scattering, the possible existence of a lower phase transition near T_m , the details of the phason coupling to the LA and TA modes, and the structural details of the incommensurate distortion.

Note added in proof: The neutron scattering investigation mentioned in the third sentence of the text is reported in Ref. 14. Those workers have recently repeated their measurements [D. E. Cox *et al.*, *Bull. Am. Phys. Soc.* **26**, 303 (1981)], and find unequivocally

that the phase below 247 K is incommensurate and, in fact, the incommensuration exhibits a slight temperature dependence well below the transition. Since our samples are from the same source as those employed by Cox *et al.*, we assume here that the phase below 247 K is incommensurate in our samples.

ACKNOWLEDGMENTS

The authors thank A. D. Bruce, H. Z. Cummins, P. A. Fleury, B. Halperin, A. P. Levanyuk, D. J. Lockwood, R. Pynn, and J. F. Scott for useful discussions of the work. One of us (K.B.L.) would like to thank J. F. Scott in particular for suggesting to him the applicability of the theory due to Bhatt and McMillan. We thank D. J. Lockwood and J. F. Scott for participating in a reciprocal sharing of unpublished data with us while both their investigations and ours were still underway. We also thank S. DiCenzo, P. A. Fleury, P. D. Laxay, and L. Schnemeyer for critical readings of the manuscript at various points during its development.

-
- ¹J. A. Wilson, F. J. DiSalvo, and S. Mahajan, *Adv. Phys.* **24**, 117 (1975).
²M. Iizumi, J. D. Axe, G. Shirane, and K. Shimaoka, *Phys. Rev. B* **15**, 4392 (1977).
³E. T. Keve, S. C. Abraham, and J. L. Bernstein, *J. Chem. Phys.* **51**, 4928 (1969).
⁴A. M. Glass, M. E. Lines, F. S. L. Hsu, and H. J. Guggenheim, *Ferroelectrics* **22**, 701 (1978).
⁵J. F. Scott, *Rep. Prog. Phys.* **42**, 1055-84 (1979).
⁶A. Janner and T. Janssen, *Phys. Rev. B* **15**, 643 (1977).
⁷K. B. Lyons, T. J. Negran, and H. J. Guggenheim, *J. Phys. C* **13**, L415 (1980).
⁸H. Cailleau, J.-L. Baudour, J. Meinel, A. Dworkin, F. Moussa, and C. M. E. Zeyen, *Faraday Discuss. Chem. Soc.* **69**, 7 (1980).
⁹I. J. Fritz, *Phys. Lett.* **51A**, 219 (1975).
¹⁰J. F. Ryan and J. F. Scott, *Solid State Commun.* **14**, 5 (1974).
¹¹Yu. A. Popkov, S. V. Petrov, and A. P. Mokhir, *Sov. J. Low Temp. Phys.* **1**, 91 (1975) [*Fiz. Nizk. Temp.* **1**, 189 (1975)].
¹²D. W. Bechtle and J. F. Scott, *J. Phys. C* **10**, L209 (1977).
¹³D. W. Bechtle, J. F. Scott, and D. J. Lockwood, *Phys. Rev. B* **18**, 6213 (1978).
¹⁴D. E. Cox, S. M. Shapiro, R. A. Cowley, M. Eibschutz, and H. J. Guggenheim, *Phys. Rev. B* **19**, 5754 (1979).
¹⁵D. J. Lockwood, A. F. Murray, and N. L. Rowell, *J. Phys. C* **14**, 753 (1981).
¹⁶K. B. Lyons and H. J. Guggenheim, *Solid State Commun.* **31**, 285 (1979).
¹⁷T. J. Negran, *Ferroelectrics* (in press).
¹⁸K. B. Lyons and P. A. Fleury, *J. Appl. Phys.* **47**, 4898 (1976).
¹⁹G. E. Devlin, J. L. Davis, I. Chase, and S. Geschwind, *Appl. Phys. Lett.* **19**, 138 (1971).
²⁰K. B. Lyons (unpublished).
²¹K. B. Lyons and P. A. Fleury, *Phys. Rev. Lett.* **37**, 161 (1976).
²²F. S. Hsu, unpublished data.
²³R. N. Bhatt and W. L. McMillan, *Phys. Rev. B* **12**, 2042 (1975).
²⁴W. L. McMillan, *Phys. Rev. B* **12**, 1197 (1975).
²⁵J. A. Wilson, F. J. DiSalvo, and S. Mahajan, *Adv. Phys.* **24**, 117 (1975).
²⁶M. L. Boriack and A. W. Overhauser, *Phys. Rev. B* **17**, 4549 (1978).
²⁷J. F. Scott, F. Habbal, and M. Hidaka (unpublished).
²⁸R. A. Cowley and A. D. Bruce, *J. Phys. C* **11**, 3577 (1978).
²⁹J. Birman (private communication). Also A. P. Levanyuk, in *Proceedings of the Fifth International Meeting on Ferroelectricity*, State College, Pennsylvania, August 17-21, 1981 (in press).
³⁰T. Natterman and J. Przystawa (private communication).
³¹P. Toledano, in *Proceedings of NATO Advanced Study Institute, Nonlinear Phenomena at Phase Transitions and Instabilities*, Geilo, Norway, April, 1981 (in press).